Mechanisms of microvoid formation within KCl single crystals in the pulse energy release area of laser focused radiation

Yu.I.Boyko[*]*, M.A.Volosyuk, V.G.Kononenko*

[*]Institute for Scintillation Materials, STC "Institute for Single Crystals", National Academy of Sciences of Ukraine, 60 Lenin Ave., 61001 Kharkiv, Ukraine V.Karazin Kharkov National University, 4 Svobody Sqr., 61022 Kharkiv, Ukraine

Mechanism of micropore formation in the area of pulse energy release of the laser focused radiation in KCl single crystals was studied experimentally at low (77 K) and room (300 K) temperatures. The pulse duration was varied from $5 \cdot 10^{-8}$ s to 10^{-3} s and pulse energy — from 1 to 20 J. The observed pore sizes were $(0.75 \div 120) \cdot 10^{-6}$ m. The dislocation structure around the pores and photo-elastic stress pattern were studied. For the experimental results obtained the following values were estimated: the initial pressure in the relaxation area $(2 \cdot 10^9 \mathrm{N/m^2})$, the heated-up "nucleus" temperature (1100 K), and the laser pulse absorbed energy corresponding to a given pore size. As it is seen from the experiments, the dislocation mechanism contribution into the substance transport for pore sizes less than 10^{-5} m is $2 \div 4$ %, while the rest of substance is taken away by crowdion (interstitial atom) mechanism. The diffusion contribution into the mass transport is found to be negligible.

Экспериментально исследован механизм образования микропор в очаге импульсного энерговыделения сфокусированного излучения лазера в монокристаллах KCl при температурах 77 К, 300 К (комнатная). Варьировались длительность импульса ($5 \cdot 10^{-8}$ s, 10^{-3} s) и энергия импульса ($1 \div 20$ Дж). Размеры наблюдавшихся пор: $(0.75 \div 120) \cdot 10^{-6}$ м. Изучена дислокационная структура вокруг пор и картина фотоупругих напряжений. Из совокупности полученных экспериментальных данных оценены начальное давление в области релаксации ($2 \cdot 10^9$ Н/м^2), температура разогретого "ядра" (1100 К) и поглощенная энергия лазерного импульса, соответствующая данному размеру поры. Вклад дислокационного механизма в процесс переноса вещества, следующий из эксперимента, для размеров пор до 10^{-5} м составляет величину ($2 \div 4$) %; остальное вещество вынесено краудионным (межузельным) механизмом. Вклад диффузии в перенос массы пренебрежимо мал.

1. Introduction

It is known that powerful enough laser pulses passing through a solid dielectric cause destructions like macrovoids and cracks [1, 2]. In super pure materials absorption of laser radiation can be provoked either by impact ionization with electrons generated by photo-ionization of defects or by multi-photon ionization of lattice atoms, or by metallization of dielectric with narrow enough band gap under high intense radiation [3]. In [4] the mechanism for initial electron generation by means of cascade Auger-transitions in alkalie-halide crystals (AHC) was proposed. In real solids containing various other-phase inclusions a mechanism of heating followed by plasma formation may act, initially, in the inclusion area, and then also in adjacent region of the crystal. For substances with narrow band gap this can be stimulated by thermal ioni-

zation of the adjacent-to-inclusion matrix. Also, a mechanism of matrix photo-ionization by UV irradiation of plasma formed from nanoinclusion substance is possible [5]. The fact that the local heating of crystal and plasma formation are activated by impurity centers, in particular, clusters of anion and cation dopes, was brought out clearly enough in [6]. In KCl single crystals grown in protective phosgene atmosphere allowed decrease the impurity content to 10^{-6} %, none of crystal bulk fracture was observed under similar and even higher intensity of laser irradiation. Experimentally measured temperatures in the fracture area are in the range from $0.55 \cdot 10^4$ to $2.7 \cdot 10^4$ degrees [1, 6].

Plastic deformation and fracture processes under optical breakdown remain insufficiently studied for the time present. In the work [7] an idea of dislocation mechanism of their generation was developed. Further investigations have shown that it is necessary to consider and study the crowdion and interstitial mechanisms as well [8−16].

In order to obtain correct and reliable evaluations of dislocation and crowdion mechanism contributions, it is necessary to study physical processes preceded the pore formation, their parameters, the kinetics of crystal cooling, and to estimate the role of diffusion processes in total mass transfer. Indeed, such problem was set by us during the experiments described below. This work is devoted to determination of mechanisms of local laser influence onto dielectric medium, which is an important problem also for physics of electromagnetic radiation interaction with substance, and for strength and plasticity physics.

2. Experimental

As investigation object we used KCl single crystals grown from melt by Kiropulos method; the initial dislocation density was ~$5 \cdot 10^5$ cm^{-2}. Parallelepipeds of $(1 \times 1 \times 2)$ cm^3 size with $\{100\}$ type sides were cut off from a large block. The laser beam was focused in the bulk of the sample using a lens with focal distance $f = 10$ cm. The beam direction coincides with $\langle 100 \rangle$ type crystallographic direction.

The main experiments were carried out using a ruby laser GOR-30 in the regime of free generation. Pulse duration $\tau = 10^{-3}$ s, energy up to 20 J, and the generated radiation wavelength $\lambda = 694$ nm were used. The samples were irradiated at 77 K and 300 K.
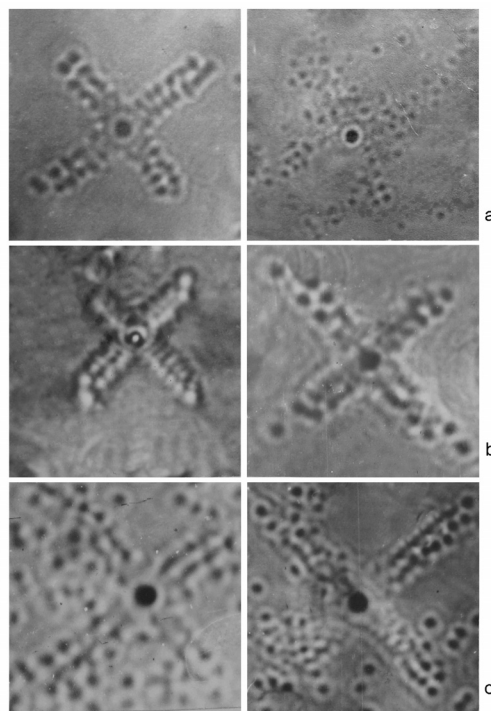

Fig. 1. Examples of micrographs of dislocation structures near pores under different experimental conditions ($\times 1000$): a) Ruby laser, free generation, $\tau = 10^{-3}$ s, T — room temperature; b) Neodymium laser modulated Q-factor, $\tau = 5 \cdot 10^{-8}$ s, T — room temperature; c) Ruby laser, free generation, $\tau = 10^{-3}$ s, $T = 77$ K.

Also, comparative experiments were carried out at $T = 300$ K with the samples irradiated using neodymium laser with modulated Q-factor ($\tau = 5 \cdot 10^{-8}$ s, $\lambda = 1054$ nm, $W \approx 1$ J).

Using pulse duration and temperature variations during irradiation we influenced on fractional participation of every mass transfer mechanism, thus, it gave a possibility to understand, what factors were crucial for realization of one or another mass transfer mechanism. After the laser irradiation the samples were cleaved by cleavage planes, and then the dislocation structure near opened voids and the photo-elastic stress pattern were studied.

3. Results and discussion

The experimentally observed pore size varied from 10^{-4} to 10^{-2} cm. In Fig. 1 typical micrographs of dislocation structures are shown. Dislocation "rays" look like the intersections of circular dislocation loops or helical dislocation by the cleavage plane. This is so-called pencil sliding which was observed in [17] for the first time. In our
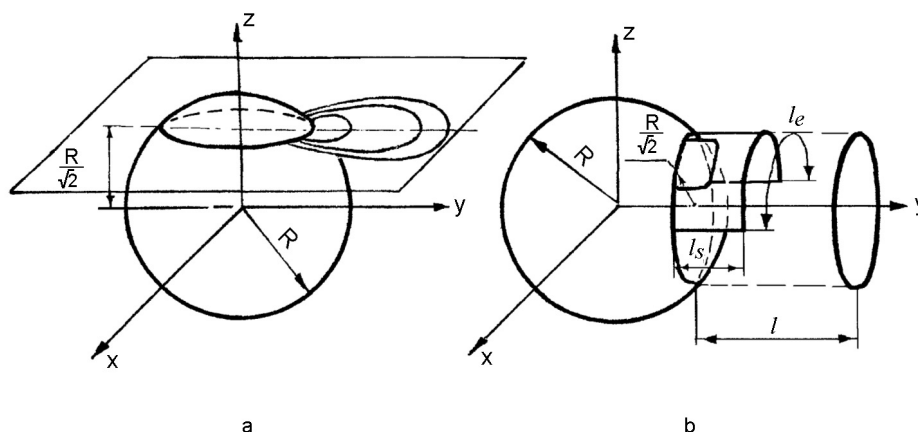
Fig. 2. Schemes of shear dislocation loop generation (a) and prismatic indentation (b) from the surface of spherical void under pressure (l_s and l_e — current length of screw and edge parts of the dislocation loop formed during prismatic indentation (pencil sliding); l — distance between generated prismatic loop and pore surface where it was born).

case this is also quite possible, if takes into consideration that in AHC besides the host sliding system in {110} type planes there is also additional one in {100} type [18]. Practically always, the process of prismatic indentation begins from thermal fluctuation generation of shear loop on the surface of a dilating inclusion (or a spherical pore under pressure) where maximum shear stress acts (Fig. 2a,b), otherwise for indentation, the screw parts of growth dislocations near inclusions are used (Fig. 3).

When a shear loop bearing by its screw component on the inclusion surface is generated, the screw components move towards one another, run round the inclusion (Fig. 2b), and generate interstitial prismatic loops and multiple-turn helicoids.

The estimations and calculations below are carried out in assumption that each of mass transfer mechanisms acts independently from each other, being determined only by external conditions and intrinsic possibilities of realization.

It is known that if isotropic solid contains a spherical void with radius R much less than the body size, and pressure P acts onto internal surface of the void, the shear stresses, e.g. the components $\sigma_{yx} = \sigma_{xy}$ acting in XOY plane (see Fig. 2b; OY axis is directed along the direction of easy sliding and possible prismatic indentation) are described by the relationship [19]:

$$\sigma_{yx} = \sigma_{xy} = \frac{3}{2} \cdot R^3 \cdot \frac{xy}{(x^2 + y^2)^{5/2}} \cdot P, \quad (1)$$
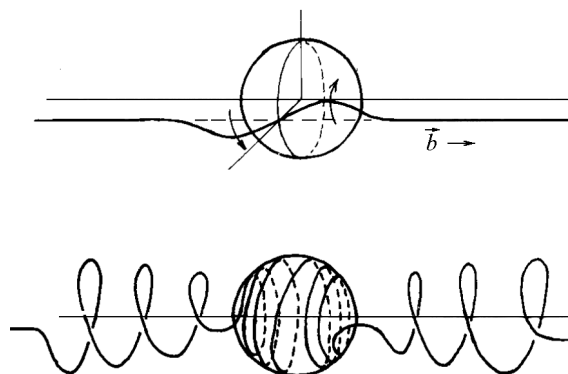
where R — radius of spherical void.

Fig. 3. Scheme of helicoid forming from the part of a screw dislocation positioned near the pore under pressure.

The shear stresses on the void surface achieve the maximum value in the point with coordinates $x = y = R/\sqrt{2}$ and in other points on the void surface which are visible from the point of origin at the angle 45° to OY axis, where dislocation loops should be generated (Fig. 2b):

$$(\sigma_{yx}^s)_{\max} = \frac{3}{4} P. \quad (2)$$

In the plane parallel to OY axis ($z = R/\sqrt{2}$) far from the pore (at $y \gg R$) the stresses σ_{yx} decrease according to the law: $\sigma_{yx} \sim (R/x)^4$.

Assuming, as in [19], the dislocation loops stop at the distance l_{dis} from the void where shear stresses drop to Pierls threshold σ_p stress level we obtain the dislocation assemblage (ray) length l_{dis} as:

Table. P_0V_0 and other parameters for selected five pore sizes

Points on the curve from Fig. 3	Pore radius, R, 10^{-6} m	Pore volume, V, m^3	P_0V_0, J	P_0, 10^9 N/m²	l_{dis}, 10^{-6} m	$dl_{dis}/d(R^{1/4})$
1	0.75	$1.77 \cdot 10^{-18}$	$2 \cdot 10^{-9}$	1.13	10.5	$2.68 \cdot 10^{-4}$
2	1.7	$2.03 \cdot 10^{-17}$	$0.32 \cdot 10^{-7}$	1.59	18	$4.9 \cdot 10^{-4}$
3	13	$9.2 \cdot 10^{-15}$	$2.11 \cdot 10^{-5}$	2.29	40	$24.8 \cdot 10^{-4}$
4	62	$9.7 \cdot 10^{-13}$	$1.7 \cdot 10^{-3}$	1.7	190	$74.3 \cdot 10^{-4}$
5	120	$7.24 \cdot 10^{-12}$	$1.5 \cdot 10^{-2}$	2.0	340	$128 \cdot 10^{-4}$

$$l_{dis} = R \left(\frac{3P}{4\sigma_p} \right)^{1/4}. \qquad (3)$$

In initial moment when the void is of R_0 size, the pressure in it is P_0. As the void expands in the pulse regime, the heat exchange can be implied absent, i.e. the swelling process is assumed adiabatic. In this case, $P_0V_0 = PV$, and the relationship (2) can be written as:

$$(\sigma_{yx}^s)_{max} = \frac{3}{4} P_0 \left(\frac{V_0}{V} \right), \qquad (4)$$

and l_{dis} is obtained in the following form:

$$(5)$$
$$l_{dis} = \left(\frac{3}{4} \frac{P_0 R_0^3}{\sigma_p} \right)^{1/4} R^{1/4} = \left(\frac{9}{16\pi} \frac{P_0V_0}{\sigma_p} \right)^{1/4} R^{1/4}.$$

In relationship (5) the experimentally measured values l_{dis} and R are interconnected. For large pores, where the dislocation ray length is difficult to resolve in the dislocation pattern, the data of stress polarization pattern were used, in which, as it was shown in [7], the ray visible length l_{opt} in ⟨110⟩ type direction is by a factor of 3.7 larger than l_{dis}. This fact was established by systematic measurements of l_{dis} and l_{opt} for the pores in the size range where both values are measurable. When the dependence l_{dis} versus $R^{1/4}$ is plotted and the tangent to the curve is drawn in some point, the slope ratio for the chosen point is:

$$\frac{dl_{dis}}{d(R^{1/4})} = \left(\frac{9}{16\pi} \frac{P_0V_0}{\sigma_p} \right)^{1/4}. \qquad (6)$$

From (6) it is possible to determine the initial parameters of the heated area (P_0V_0) for the void corresponding to the point chosen in the curve $l_{dis}(R^{1/4})$ at the known σ_p value. The dependence l_{dis} versus $R^{1/4}$ is
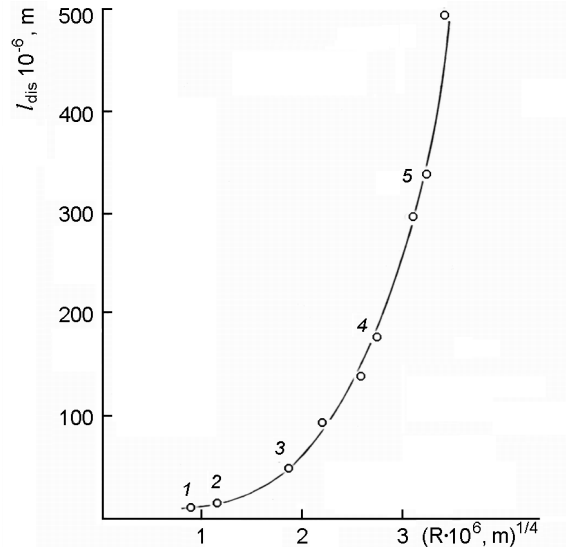

Fig. 4. Dependence l_{dis} on $R^{1/4}$ (figures 1–5 indicate the points for which the slope ratios were determined and parameters P_0V_0 were calculated, see Table 1).

shown in Fig. 4, and the calculated P_0V_0 and other parameters for chosen five pore sizes (marked in Fig. 4) are given in Table.

The following conclusions can be made from the data above. First, during formation of the raptures observed only a minor part of the pulse energy, $10^{-9} \div 10^{-2}$ J, is absorbed that evidently explains the absence of any correlation between the pulse energy and the rapture character. Second, after changing void size more than by two orders of value the initial pressure within them remains practically stable and equal to shear ultimate stress $P \simeq 2.0 \cdot 10^9$ N/m² for crystals. The author of [6] also came to conclusion that the formation of plasma at 5500 K under pressure of an order of 10^9 N/m² precedes to the fractures formation.

Let us estimate the temperature of the heated area (a nucleus). The nucleus volume relative variation $\delta V/V$ and the pressure necessary to restrain it are related as:

$$\frac{\delta V}{V} = \frac{P}{K}, \qquad (7)$$

where K — volume elasticity modulus (for KCl crystal, $K = 1.74 \cdot 10^{10}$ N/m^2 [20], $P \approx 2 \cdot 10^9$N/m^2). On the other hand:

$$\frac{\delta V}{V} = 3\alpha\Delta T, \qquad (8)$$

where α — linear expansion coefficient, which is $\alpha = 48 \cdot 10^{-6}$ deg^{-1} for KCl; ΔT — the body temperature variation. From (8) taking (7) into consideration it follows:

$$\Delta T = \frac{\delta V/V}{3\alpha} \approx 800(K). \qquad (9)$$

Thus, if the experiment is carried out at room temperature, $T \simeq 300$ K, the temperature of the heated nucleus is about 1100 K and it is practically the same for all pores with sizes in the range of the study (from 10^{-4} cm to 10^{-2} cm).

Plasma cloud size, plasma temperature, amount of absorbed by it energy from the laser pulse, and time interval of plasma burning significantly depend on physical properties and sizes those extrinsic particles which fall within the focal area of the laser pulse in the moment of irradiation. The conclusion about plasma extinction follows from the fact that in all of described experiments, only a minor part of the pulse energy is found to be utilized for crystal fracture (see Table). Moreover, according to the literature data [21, 22], as the pressure rise exceeds $100 \div 200$ atm., the radiation losses increase quickly, thus, result in optical breakdown threshold increasing that, in turn, leads to plasma extinction.

Using the micrographs like given in Fig. 1, it is easy to calculate the number of visible interstitial dislocation loops, their sizes, total amount near each pore, and, taking into account all the easy sliding directions to estimate the substance volume brought out by the loops from the void. It turned out that this is only not more than $(2 \div 4)$ % of the generated pore volume. This fact may signify that either emitted dislocation loops are dissolved by diffusion meanwhile the high temperature exist in the crystal, or the main volume of substance is brought out by the mechanism of crowdion (interstitial) migration of atoms.

To estimate diffusion fluxes, it is necessary to know the temperature distribution about a pore and its time variation. The task is reduced to solution of the heat-conductivity equation for isotropic three-dimensional body of radius L with centered within it heated small spherical nucleus of radius $r_0 \ll L$:

$$\frac{\partial T}{\partial t} = a^2 \Delta T, \qquad (10)$$

where Δ is Laplacian. Initial and boundary conditions are the follows $T(r,0) = f(r)$, $T(L,t) = 0$. Temperature conductivity is $a^2 = k/(c \cdot \rho)$, with k — heat conductivity, ρ — density, and c — specific heat. Function $f(r)$ describes the temperature distribution in the body at the instant of time $t = 0$. In our case, the initial condition comes to the fact that at $t = 0$ instant, in the sample center (in the lens focal area) there take place absorption of a part of the laser pulse energy and sharp increase of the temperature up to some value T_0 in the crystal area of r_0 radius.

The initial condition is not known exactly. To analyze the temperature distribution we apply the solution for the case of an instant point heat source in the center of the body in which the heat amount Q is injected at the instant $t = 0$, at that the temperature of the crystal heated volume (υ becomes $T_0 = Q/(\upsilon c\rho)$. The solution of equation (10) is described as following [23]:

$$T(r,T) = \frac{T_0}{(2a\sqrt{\pi t})^3} \exp - \left[\frac{(r - r_0)^2}{4a^2 t}\right]. \qquad (11)$$

According to (11) in any flock of points at the distance r from the center the temperature increases in the beginning, achieves the maximum, and then decreases with time. This maximum moves from the crystal center (the center of energy release) quickly falling by its height. The process rate is determined by the crystal temperature conductivity. As it follows from (11) the distance to some point of observation, r, the time period, t, after which the temperature maximum will be achieved in this point, and the temperature conductivity, a^2, are related by the expression:

$$r^2 = 4a^2 t. \qquad (12)$$

In the point of a heat pulse injection, at $t > 0$ the Gaussian temperature maximum is formed. During heat propagation in the crystal the height of the maximum decreases with time by the law: $T_{max} \sim 1/(\sqrt{t})^3$.

Radius of the pore surrounded by dislocation loops is equal to the dislocation ray length l_{dis} corresponding to the pore size. From equation (12) we find the time period t_m, in which the temperature maximum will be achieved on the surface of a sphere surrounding the crystal region of ldis radius. For pores 1–5 given in Table, we obtain the following evaluations: $t_{m1} = 2.8 \cdot 10^{-5}$ s, $t_{m2} = 8 \cdot 10^{-5}$ s, $t_{m3} = 4 \cdot 10^{-4}$ s, $t_{m4} = 9 \cdot 10^{-3}$ s, $t_{m5} = 2.5 \cdot 10^{-2}$ s.

The average temperature in the relaxation region of radius l_{dis} can be evaluated using the energy conservation law and data from Table 1 about the energy absorbed by the crystal during formation of the pore of a given size:

$$\langle T \rangle = \frac{P_0 V_0}{V_{dis} \cdot \rho c}, \qquad (13)$$

where $V_{dis} = (4/3)\pi l_{dis}^3$; $\rho = 2.4 \cdot 10^3$ kg/m^3 is KCl density; $c = 5.77 \cdot 10^2$ J/(kg·deg). Substituting the values for points 1–5 from Table we obtain: $\langle T_1 \rangle = 0.35$ deg, $\langle T_2 \rangle = 1.11$ deg, $\langle T_3 \rangle = 67$ deg, $\langle T_4 \rangle = 50$ deg, $\langle T_5 \rangle = 77$ deg.

Of course, the errors in these evaluations are rather high, especially for estimations of the average temperature in the relaxation zone. The equation (13) contains two measured values which errors are added up. Nevertheless, these evaluations allow quite logical conclusions. First, if the energy absorbed is bigger, the relaxation region heating temperature is higher; and second, if the relaxation region is bigger, the more time is needed for it heating and the longer time is required for its cooling. Thus, the contribution of diffusion processes under high local energy release when a large pore is formed will be evidently larger.

Let us evaluate the diffusion flux from the loops being dissolved. Based on the estimations above the temperature can be taken as not more than 100 degrees higher than room value (i.e. $T \simeq 400$ K) in the crystal relaxation region. The loop dissolution flux can be calculated using the relationship for the interstitial loop collapse [24]:

$$\frac{dR_l}{dt} = \qquad (14)$$

$$= \frac{2\pi}{b\ln(8R_l/b)} \left[\frac{Gb(\ln(R_l/b) + g)D_i C_i \omega}{4\pi(1 - \nu)kTR_l} + D_\upsilon \Delta C_\upsilon \right],$$

where D_υ, D_i are diffusion coefficients for vacancies and interstitials, respectively, at

temperature T; G is shear modulus; ν is Poisson coefficient; b is Burgers vector; R_l is loop radius; k — Boltzmann; ω — atomic volume; ΔC_υ — vacancy supersaturation far from the loop; C_i — equilibrium concentration of interstitials far from the loop; $g \simeq 2 \div 3$ takes into account the energy of dislocation nucleus.

The loop volume is $V_l = \pi R_l^2 b$. Taking into consideration only the first summand in the equation (14) and the fact that $(\ln (R_l/b) + g)$ and $\ln(8R_l/b)$ are of the same order of value for the flux of atoms from the dislocation loop, we obtain:

$$\frac{dV_l}{dt} \approx -\frac{\pi GbD\omega}{(1 - \nu)kT}. \qquad (15)$$

Substituting the appropriate values: $G = 10^{10}$ N/m^2, $b \simeq 3 \cdot 10^{-10}$ m, $\omega = 3 \cdot 10^{-29}$ m^3, $k = 1.38 \cdot 10^{-23}$ J/deg, $T = 400$ K, $\nu \approx 0.3$, and the activation energy of KCl self-diffusion $E_s = 2.1 \div 2.4$(eV) [20, 25] we obtain $dV_l/dt = 4 \cdot 10^{-35}$(m^3/s). Thus, the diffusion flux of the loop dissolution is negligible.

The question is: why the dislocation transfer mechanism being quite perfect energetically becomes less effective than the crowdion one in the experimental case described? Perhaps, the point is that the mechanisms discussed have substantially different specific relaxation times. In order to form a loop, it is necessary to shift one crystal part relative to another by Burgers vector. For a crowdion to be formed, only one atom should be shifted to the required position. That's why in pulse processes the crowdion mechanism becomes more preferable. At that the crowdion turns into a mobile particle with low effective mass [26]. So, in [27] it is shown that crowdion in copper, for instance, has effective mass only 0.23 of atom mass, while its localization level overlaps 3–4 lattice parameters along the close-packed row. These parameters predetermine high mobility and "inertial-less" ability of crowdions in the mass transfer mechanism. Additionally, in [28] it was shown that the crowdion high dynamics is stimulated by strongly non-uniform field of elastic strains with high gradients that is in our case.

At temperature 77 K the dislocation structure exists near pores, but it substantially differs qualitatively. At "nitrogen" temperatures the dislocation "rays" end, as a rule, by a "cap" of scattered etching pits. Schematically, this phenomenon can be ex-

plained as follows. As the temperature decreases crowdion mobility rises sharply, and being under the stress field they rather easy (without conversion) move away from the pore at the identical distance (and in the same direction) that the dislocation loops move. Due to low temperature the supersaturation of lattice by interstitial atoms takes place. Under heating to room temperature this supersaturation is partially relaxed at the expense of occurring interstitial dislocation loops which are revealed under etching as the "caps" of etching pits in specific crystallographic directions. This also supports the fact that under conditions described it is the crowdions were substance carriers which generated and moved in close-packed directions.

In ion crystals the crowdions must be generated and move simultaneously in cation and anion sublattices, and, obviously, there should exist a self-regulation mechanism inhibiting the charge space separation in macroscale and the dielectric polarization. One of the possibilities to avoid polarization is the formation of crowdion dipole consisting of an anion and a cation being connected with each other and moving as a single whole. If to a zero approximation, the crowdion dipole is taken as an "electrically neutral" formation moving in a "tube" of an electrically neutral crystal and interacting with nearest neighbors only without taking into account the long-range Coulomb forces, all the conclusions of [26−29] concerning the crowdion effective mass, its localization extent, character of influence of crystal stress state type and its evolution on the crowdion dynamics which are valid for cryogenic crystals and metals can be applied to ion crystals as well.

The experiments do not contradict such conclusion and even indicate high activity of the crowdion mass transfer mechanism during pore formation under conditions of optical breakdown of ion crystals.

4. Conclusions

The micropore formation in KCl single crystals was studied in the area of pulse energy release of laser focused radiation at the crystal temperatures 77 K and 300 K and the laser pulse durations 10^{-3} s and $5 \cdot 10^{-8}$ s. The range of observed pore sizes overlaps the area by $(0.75 \div 120) \cdot 10^{-6}$ m.

Using the experimental results the initial pressure in the dilation area was evaluated $\sim 2 \cdot 10^9$ N/m^2 found to be practically similar for all the pore sizes, the

temperature of the crystal heated area (nucleus) being $T_{cr} + 800$ K (T_{cr} is the crystal temperature in the experiment). The value of absorbed laser pulse energy depending on the formed pore radius was estimated. Based on the solution analysis of the heat conductivity equation describing the crystal cooling after a local temperature outburst, the diffusion contribution into substance transfer process was estimated and found to be negligible.

From the experimental data and the theoretical estimation it is follows that under conditions described during pore formation up to the sizes of the order 10^{-5} m, the main substance transport mechanism is the crowdion one (96−98 %). The leading role of the crowdion mechanism becomes apparent also in formation of etching pit "caps" on dislocation "rays" at low temperatures as a result of relaxing the supersaturation of the lattice by interstitial atoms in these zones of the crystal. The predominant role of the crowdion mechanism under experimental conditions described, evidently, is caused by combination of such facts as high impulsivity of the stress relaxation process around the heated region of the crystal, purely shear character of deformation in stressed area, highly inhomogeneous strains (high gradients), and low temperatures of the experiments.

References

1. L.M.Belyaev, A.N.Golovastikov, V.V.Nabatov, *Fiz. Tverdogo Tela*, **10**, 3733 (1968).

2. G.I.Barenblatt, *Zh. Eksper. Teor, Fiz.*, **54**, 1337 (1968).

3. S.V.Karpenko, A.Kh.Kyarov, A.I.Temrakov, D.L.Vinokurov, *Kristallografia*, **47**, 326 (2002).

4. V.D.Kulikov, *Zh.Teor, Fiz.*, **79**, 60 (2009).

5. V.G.Kononenko, A.K.Yemets, *Ukr. Fiz. Zh.*, **22**, 1378 (1977).

6. V.E.Rogalin, in: Collected Articles "Laser Optical Systems and Technologies", FGUP "NPO Astrofizika", Moscow (2009), p.70.

7. Ya.E.Geguzin, A.K.Yemets, V.G.Kononenko, *Fiz. Tverdogo Tela*, **17**, 2984 (1975).

8. J. Frenkel, T.Kontorova, *J.Phys.*, **1**, 137 (1939).

9. H.R.Paneth, *Phys. Rev.*, **80**, 708 (1950).

10. V.L.Indenbom, *Zh. Eksper. Teor, Fiz.*, **12**, 526 (1970).

11. V.L.Indenbom, A.N.Orlov, *FMM*, **43**, 469 (1977).

12. V.N.Rozhansky, N.L.Slyozov, A.A.Urusov-skaya, *Fiz. Tverdogo Tela*, **13**, 411 (1971).

13. Yu.I.Golovin, A.I.Tyurin, *FTT*, **42**, 1818 (2000).

14. Z.K.Saralidze, M.V.Galustashvili, D.G.Driaev, *Phys. Solid State*, **48**, 1298 (2006).

15. V.G.Kononenko, *Metallofizika*, **7**, 71 (1985).

16. Yu.I.Boyko, Ya.E.Geguzin, A.K.Yemets, *Fiz. Tverdogo Tela*, **13**, 3096 (1971).

17. D.A.Jones, S.W.Mittchell, *Phyl. Mag.*, **3**, 1 (1958).

18. J.Hirth, J.Lothe, Theory of Dislocations, McGraw-Hill, New York (1968).

19. Ya.E.Geguzin, V.G.Kononenko, *Fiz. Tverdogo Tela*, **15**, 3550 (1973).

20. Ch.Kittel, Introduction to Solid State Physics, Fourth Eddition, John Wiley and Sons. Inc., New York-London-Sydney-Toronto.1956

21. Yu.P.Raizer, *Usp.Fiz.Nauk*, **132**, 549 (1980).

22. G.V.Ostrovskaya, A.N.Zaidel, *Usp.Fiz.Nauk*, **111**, 579 (1973).

23. A.N.Tikhonov, A.A.Samarsky, Equations of Mathematical Physics, Nauka, Moscow (1972) [in Russian].

24. A.M.Kosevich, E.K.Saralidze, V.V.Slyozov, *Fiz. Tverdogo Tela*, **6**, 3383 (1964).

25. A.Lidiard, Ionic Conductivity, Handbuch der Physik, Dand XX, Tell II, S.246 (1957).

26. A.M.Kosevich, Physical Mechanics of Real Crystals, Naukova Dumka, Kiev (1981) [in Russian].

27. V.D.Natsik, S.N.Smirnov, E.I.Nazarenko, *FNT*, **27**, 1295 (2001).

28. V.D.Natsik, E.I.Nazarenko, *Fiz. Nizkikh Temp.*, **26**, 283 (2000).

29. V.D.Natsik, S.N.Smirnov, *Kristallografia*, **54**, 1034 (2009).

Механізми формування мікропорожнин у монокристалах KCl в очагу імпульсного енерговиділення сфокусованого лазерного випромінювання

Ю.І.Бойко, М.А.Волосюк, В.Г.Кононенко

Експериментально досліджено механізм утворення мікропор в очагу імпульсного енерговиділення сфокусованого випромінювання лазера у монокристалах KCl при температурах 77 К, 300 К (кімнатна). Варіювалися тривалість імпульсу ($5{\cdot}10^{-8}$ с, 10^{-3} с) і енергія імпульсу ($1 \div 20$ Дж). Розміри пор, що спостерігалися: $(0.75 \div 120){\cdot}10^{-6}$ м. Вивчено дислокаційну структуру навколо пор і картину фотопружних напружень. Із сукупності отриманих експериментальних даних оцінено початковий тиск в області релаксації ($2{\cdot}10^{9}$ Н/м^2), температуру розігрітого "ядра" (1100 К) і поглинену енергію лазерного імпульсу, відповідну даному розміру пори. Внесок дислокаційного механізму в процес перенесення речовини, що слідує з експерименту, для розмірів пор до 10^{-5} м складає величину $(2 \div 4)$ %; решта речовини винесена краудіонним (міжвузельним) механізмом. Внесок дифузії у перенесення маси нехтовно малий.